

## Application of Zach Phase Plates for Phase-Contrast Transmission Electron Microscopy: Status and Future Experiments

S. Hettler<sup>1</sup>, J. Wagner<sup>1</sup>, M. Dries<sup>1</sup>, M. Oster<sup>2</sup>, R.R. Schröder<sup>2</sup>, D. Gerthsen<sup>1</sup>

<sup>1</sup> Laboratory for Electron Microscopy, Karlsruhe Institute of Technology, D-76128 Karlsruhe, Germany

<sup>2</sup> BioQuant CellNetworks, University of Heidelberg, Im Neuenheimer Feld 267, D-69120 Heidelberg, Germany

Achieving phase contrast for weak-phase objects has been the driving force for the development of physical phase plates (PP) for transmission electron microscopy (TEM). Thin-film PPs have meanwhile reached a well-developed state [1]. However, carbon-based PPs suffer from fast material degradation under intense electron irradiation which has initiated the evaluation of alternative materials [2] and other PP approaches as reviewed in [3]. In contrast to thin-film PPs, electrostatic PPs allow the variation of the phase shift which opens the possibility to optimize phase contrast for different types of specimens and facilitate, e.g., wave-function reconstruction not only of weak-phase objects [4]. Among the different electrostatic PP approaches, the Zach PP [5] appears to be most promising because it minimizes obstructing structures in the back focal plane (BFP) and, hence, artifacts induced by blockade of spatial frequencies. Substantial improvements have been made with respect to contamination and charging which yields phase-contrast TEM images with well-controlled phase shift. This was demonstrated by Frindt *et al.* [6] where imaging with a Zach PP yielded for the first time in-focus phase-contrast images of weak-phase objects (filamentous actin embedded in vitreous ice) with negligible artifacts.

The benefits of the Zach PP compared to the Boersch PP are illustrated by simulations in Fig. 1. The structure of the Boersch PP (for dimensions see caption of Fig. 1) is shown in Fig. 1a. A phase shift of  $\pi/2$  was assumed for the zero-order beam. The phase shift of the Zach PP  $\phi_{pp}$  in the BFP of the objective lens of a ZEISS 912 Omega (electron energy 80 keV, focal length 3.6 mm, spherical aberration coefficient  $C_s = 2.7$  eV) is displayed in Fig. 1b. The electrostatic potential and corresponding  $\phi_{pp}$  distribution was calculated for the dimensions of a real Zach-PP structure and an applied voltage  $U = 1$  V by finite-element calculations which yields  $\phi_{pp} = \pi/2$  for the zero-order beam. The test wave function (Fig. 1c) is assumed to consist of nanoparticles (NPs) with sizes between 8 and 16 nm which induce phase shifts between  $0.25\pi$  and  $0.4\pi$ . The simulated in-focus image for the Boersch PP (Fig. 1d) shows NP contrast which is dominated by artifacts. Contrast oscillations can be recognized due to the abrupt transition between fully blocked and transmitted spatial frequencies. Artifacts are substantially reduced in the image for the Zach PP (Fig. 1e). Contrast oscillations do not occur which can be understood by the continuous  $\phi_{pp}$  change in the vicinity of the zero-order beam. Spatial frequencies are only blocked in a comparably small region of the BFP leading to slight singleside-band contrast. The bright fringe around the NPs results from the asymmetrical  $\phi_{pp}$  distribution. The contrast can be further enhanced if a microscope with a larger focal length of 15 mm is assumed as shown in Fig. 1f.

Fig. 2 shows Zach-PP TEM images of Au NPs on amorphous carbon film taken at a defocus of -375 nm and the corresponding diffractograms. Different applied voltages yield  $\phi_{pp} = 0.6\pi$  (Fig. 2a,d),  $\phi_{pp} = -0.1\pi$  (Fig. 2b,e) and  $\phi_{pp} = -0.4\pi$  (Fig. 2c,f). The contrast of the NPs can be well controlled leading to a contrast inversion from dark to bright. It is noted that the ZEISS 912 Omega is operated with a standard LaB<sub>6</sub> cathode. Further experiments are under way to study the effect of inelastic scattering on phase contrast [7].

## References:

- [1] R Danev and K Nagayama, *Ultramicroscopy* **111** (2011), p. 1305.  
 [2] M Marko *et al.*, *J. Struct. Biol.* **184** (2013), p. 237.  
 [3] R M Glaeser, *Rev. Sci. Instruments* **84** (2013), 111101.  
 [4] B Gamm *et al.*, *Ultramicroscopy* **110** (2010), p. 807.  
 [5] K Schultheiss *et al.*, *Microsc. Microanal.* **16** (2010), p. 785.  
 [6] N. Frindt *et al.*, *Microsc. Microanal.* **20** (2014), p. 175.  
 [7] Acknowledgement: Financial support by German Research Foundation (DFG) under contract Ge 841/16 and Sch 424/11.

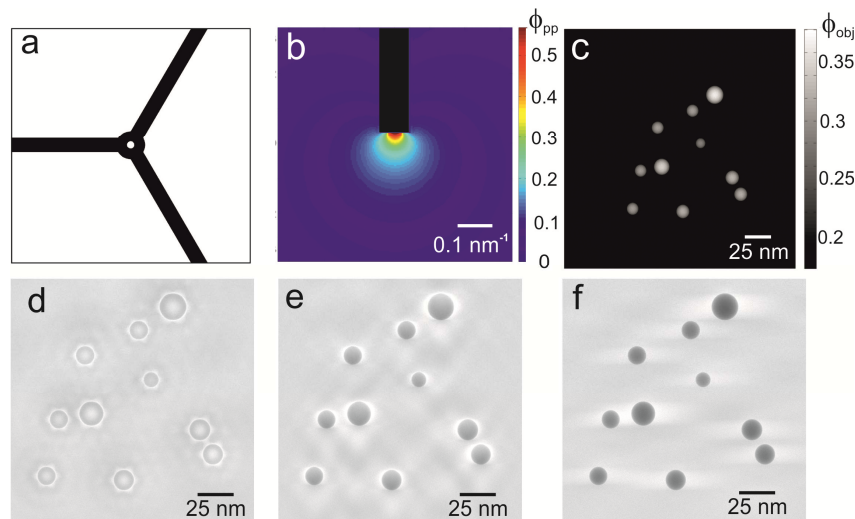
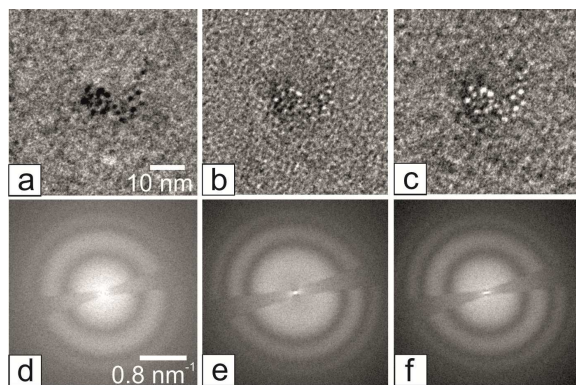


Figure 1. a) Scheme of a Boersch PP with an outer diameter of the einzel lens of 3  $\mu\text{m}$ , inner diameter of 0.8  $\mu\text{m}$  and 1.5  $\mu\text{m}$  supporting bar width, b) color-coded phase shift  $\phi_{\text{pp}}$  of the Zach PP plotted in the BFP of the ZEISS 912 Omega for a focal length of 3.6 mm and 80 keV, c) test wave function with gray-scale coded object phase shift  $\phi_{\text{obj}}$ . Simulated in-focus images for d) the Boersch PP, e) the Zach PP, and f) the Zach PP and an increased focal length of 15 mm.



**Figure 2.** 120 keV Zach-PP TEM images of Au NPs on amorphous carbon film and corresponding diffractograms taken with different applied voltages  $U$

a),d)  $U = -2 \text{ V}$  and  $\phi_{\text{pp}} = 0.6\pi$ ,

b),e)  $U = 0 \text{ V}$  and  $\phi_{\text{pp}} = -0.1\pi$ ,

c),f)  $U = 1 \text{ V}$  and  $\phi_{\text{pp}} = -0.4\pi$ .

The images are taken at a defocus of  $-375 \text{ nm}$ . The large defocus was chosen to achieve minimum NP contrast for  $U = 0 \text{ V}$ .